厚生労働科学研究委託費

革新的がん医療実用化研究事業

難治がんに対する動体追尾放射線治療の臨床評価に関する研究

平成26年度 委託業務成果報告書

業務主任者 **平岡 眞寛**

平成27（2015）年 3月

委託業務成果報告書目次

厚生労働科学研究委託費（革新的がん医療実用化研究事業）
委託業務成果報告 （総括）

難治がんに対する動体追尾放射線治療の臨床評価に関する研究

研究要旨
本研究では動体追尾放射線治療の臨床適用を一般化することを目標とし、同治療の多施設共同臨床試験を行う。当初は早期肺がんおよび局所進行膵がんを対象としていたが、肝臓がんも対象に加えることとした。臨床試験プロトコールの策定を進めるとともに、各施設治療装置が試験参加に十分な精度を有していることを確認した。

臨床試験プロジェクト
a. プロジェクトの総合推進
担当責任者：平岡　眞寛　京都大学医学部　教授
b. 臨床試験プロトコール策定
担当責任者：溝脇　尚志　京都大学医学部　准教授
c. 症例登録の開始
担当責任者：松尾　幸憲　京都大学医学部　講師
小久保　雅樹　先端医療センター病院　放射線治療科 部長
唐澤　克之　東京都立駒込病院放射線診療科治療部 部長
医学物理プロジェクト
担当責任者：中村　光宏　京都大学医学部　講師

A. 研究目的
本研究では動体追尾放射線治療の臨床適用を一般化することを目標とし、同治療の多施設共同臨床試験を行う。

B. 研究方法
臨床試験プロジェクトでは、試験プロトコールの策定を行う。医学物理プロジェクトでは、第三者機関による治療装置の出力線量測定を実施するとともに、施設間での治療手順の標準化および動体追尾精度の検証を行う。

(倫理面への配慮)
臨床試験プロトコールはヘルシンキ宣言並びに人を対象とする医学系研究に関する倫理指針に準拠して立案し、施設倫理委員会に諮問を行う。

C. 研究結果
2回の合同会議(2014/8/8、2014/11/29)並びにメールでのディスカッションと通して、肺癌に対する動体追尾照射、膵臓癌に対する動体追尾 IMRT の多施設前向き臨床試験計画を立案し、主たる研究機関である京都大学の医の倫理員会にプロトコールを提出した。同時に、肝臓癌に対する動体追尾照射の単アームの早期第 2 相試験も追加で実施することを第 2 回会議で決定し、プロトコール立案をほぼ終了した。
医学物理プロジェクトにおける「第三者機関による治療装置の出力線量測定」では、全施設で合格通知を受け取った。施

設間で治療手順に違いがあることが判明したため、治療手順の標準化を図り、臨床試験プロトコールに反映した。

D. 考察

試験デザインを実行可能性試験から早期第2相試験の形式とできたことより、試験結果のインパクトが大幅に上昇することが期待できる。出力線量測定結果より、共同試験に参加を表明している施設の線量計算精度は同等であることがわかった。

E. 結論

臨床試験プロトコールの策定を進めるとともに、各施設治療装置が試験参加に十分な精度を有していることを確認した。

F. 健康危険情報

無し

G. 研究発表

1. 論文発表

① Nakamura M, Akimoto M, Ono T, Nakamura A, Kishi T, Yano S, Nakata M, Itasaka S, Mizowaki T, Shibuya K, Hiraoka M. Interfraction Positional Variation in Pancreatic Tumors using Daily Breath-hold Cone-beam Computed Tomography with Visual Feedback. J Appl Clin Med Phys. (in press).

② Akimoto M, Nakamura M, Mukumoto N, Yamada M, Tanabe H, Ueki N, Kaneko S, Matsuo Y, Mizowaki T, Kokubo M, Hiraoka M. Baseline correction of a correlation model for improving the prediction accuracy of infrared marker-based dynamic tumor tracking. J Appl Clin Med Phys. (in press).

③ Nakamura M, Akimoto M, Mukumoto N, Yamada M,Tanabe H, Ueki N, Matsuo Y, Mizowaki T, Kokubo M,Hiraoka M. Influence of the correlation modeling period on the prediction accuracy of infrared marker-based dynamic tumor tracking using a gimbaled X-ray head. Physica Medica, 2015 (in press).

④ Shintani T, Masago K, Takayama K, Ueki K, Kimino G, Kosaka Y, Imagumbai T, Katakami N, Kokubo M: Stereotactic body radiotherapy for synchronous primary lung cancer: clinical outcome of 18 cases. Clinical Lung Cancer, (in press).

⑤ Matsuo Y, Chen F, Hamaji M, Kawaguchi A,Ueki N, Nagata

Y, Sonobe M, Morita S, Date H, Hiraoka M. Comparison of long-term survival outcomes between stereotactic body radiotherapy and sublobar resection for stage I non-small-cell lung cancer in patients at high risk for lobectomy: A propensity score matching analysis. Eur J Cancer. 2014;50(17):2932–8.

⑥ Matsuo Y, Ueki N, Takayama K, Nakamura M, Miyabe Y, Ishihara Y, Mukumoto N, Yano S, Tanabe H, Kaneko S, Mizowaki T, Monzen H, Sawada A, Kokubo M, Hiraoka M. Evaluation of dynamic tumour tracking radiotherapy with real-time monitoring for lung tumours using a gimbal mounted linac. Radiother Oncol. 2014;112(3):360–4.

⑦ Ishihara Y, Sawada A, Nakamura M, Miyabe Y, Tanabe H, Kaneko S, Takayama K, Mizowaki T, Kokubo M, Hiraoka M. Development of a dose verification system for Vero4DRT using Monte Carlo method. J Appl Clin Med Phys. 2014;15:160-172

⑧ Shiinoki T, Sawada A, Ishihara Y, Miyabe Y, Matsuo Y, Mizowaki T, Kokubo M, Hiraoka M. Dosimetric impact of gold markers implanted closely to lung tumors: a Monte Carlo simulation. J Appl Clin Med Phys. 2014;15:71-79.

2. 学会発表

① Y. Iizuka, N. Ueki, Y. Ishihara, M. Akimoto, H. Tanabe, K. Takayama, N. Mukumoto, M. Nakamura, Y. Miyabe, S. Kaneko, Y. Matsuo, T. Mizowaki, H. Monzen, A Sawada, M. Kokubo, M. Hiraoka. Evaluation of dose distribution and tracking accuracy in dynamic tumor-tracking irradiation for liver tumors using a gimbaled linac. ASTRO 56th annual meeting. Sep. 14-17, 2014. San Francisco, the US.

② 飯塚裕介、松尾幸憲、石原佳知、秋元麻未、田邊裕朗、高山賢二、植木奈美、横田憲治、溝脇尚志、小久保雅樹、平岡眞寛. Vero4DRT を用いた肝腫瘍に対する動体追尾定位放射線治療(ポスター) 日本放射線腫瘍学会 第 27 回学術大会 平成 26 年 12 月 13 日. 横浜

③ 待鳥裕美子、木藤哲史、柴田友紀子、影山俊一郎、村田裕人、清水口卓也、田中寛、藤井元彰、

二瓶圭二、唐澤克之.
Vero4DRTによる動体追尾照射を用いた肺定位放射線治療の初期経験(ポスター) 日本放射線腫瘍学会 第27回学術大会平成26年12月13日. 横浜

④ 木藤哲史、岡野智行、橋本俊信、米川五朗、古谷智久、橋本慎平、二瓶圭二、唐澤克之. 4次元放射線治療における基準マーカ位置の評価方法(口頭) 日本放射線腫瘍学会 第27回学術大会平成26年12月13日. 横浜

H. 知的財産権の出願・登録状況(予定を含む)

1. 特許取得

なし

2. 実用新案登録

なし

3. その他

なし

厚生労働科学研究委託費（革新的がん医療実用化研究事業）
委託業務成果報告

難治がんに対する動体追尾放射線治療の臨床評価に関する研究
業務項目：臨床試験プロジェクト

a. プロジェクトの総合推進
担当責任者：平岡　眞寛　　京都大学医学部　教授
b. 臨床試験プロトコール策定
担当責任者：溝脇　尚志　　京都大学医学部　准教授
c. 症例登録の開始
担当責任者：松尾　幸憲　　京都大学医学部　講師
小久保　雅樹　先端医療センター病院　放射線治療科 部長
唐澤　克之　　東京都立駒込病院放射線診療科治療部 部長

研究要旨
動体追尾治療の有効性と安全性を評価するための多施設前向き臨床試験計画を立案した。当初は肺および膵臓の２臓器を対象とし、実行可能性試験の形式を予定していたが、肝臓を追加した３臓器を対象とし、また単アームの早期第２相試験の形式に変更することとした。肺がんおよび膵がんの試験プロトコルが倫理審査中である。

A. 研究目的

動体追尾治療が臨床治療として広く展開しうるか実現可能性を評価するために、多施設前向き臨床試験計画を立案し実施する。

B. 研究方法

Vero4DRTを運用し動体追尾照射を実施している京都大学医学部附属病院、先端医療センター病院、がん・感染症センター都立駒込病院で多施設前向き臨床試験を立案・実施する。

(倫理面への配慮)

立案プロトコールは、ヘルシンキ宣言並びに人を対象とする医学系研究に関する倫理指針に準拠して立案し、各施設の医の倫理委員会の承認を得て実施する。

C. 研究結果

２回の合同会議（2014/8/8、2014/11/29）並びにメールでのディスカッションと通して、肺癌に対する動体追尾照射、膵臓癌に対する動体追尾 IMRT の多施設前向き臨床試験計画を立案し、京都大学医の倫理員会にプロトコールを提出した。プロトコールデザインは、各施設の追尾照射の臨床経験が予定よりも蓄積されていることが判明したため、当初の予定の単アームの実行可能性試験から単アームの早期第２相試験の形式に変更した。同時に、肝臓癌に対する動体追尾照射の単アームの早期第２相試験も追加で実施することを第 2 回会議で決定し、プロトコール立案をほぼ終了した。

D. 考察

試験デザインを実行可能性試験から早期第 2 相試験の形式とできたことより、試験結果のインパクトが大幅に上昇することが期待できる。

E. 結論

当初予定した肺癌に対する動体追尾照射、膵臓癌に対する動体追尾 IMRT の多施設前向き臨床試験計画を立案し、倫理委員会に提出した。来年度早々の登録開始が可能と考えられる。また、肝臓癌に対する動体追尾照射に関する臨床試験プロトコールも、来年度前半までに倫理委員会の承認を得て登録開始できる見込みである。

F. 研究発表

1. 論文発表

① Shintani T, Masago K, Takayama K, Ueki K, Kimino G, Kosaka Y, Imagumbai T, Katakami N, Kokubo M: Stereotactic body radiotherapy for synchronous primary lung cancer: clinical outcome of 18 cases. Clinical Lung Cancer, (in press).

② Matsuo Y, Chen F, Hamaji M, Kawaguchi A,Ueki N, Nagata Y, Sonobe M, Morita S, Date H, Hiraoka M. Comparison of long-term survival outcomes between stereotactic body radiotherapy and sublobar resection for stage I non-small-cell lung cancer in patients at high risk for lobectomy: A propensity score matching analysis. Eur J Cancer. 2014;50(17):2932–8.

③ Matsuo Y, Ueki N, Takayama K, Nakamura M, Miyabe Y, Ishihara Y, Mukumoto N, Yano S, Tanabe H, Kaneko S, Mizowaki T, Monzen H, Sawada A, Kokubo M, Hiraoka M. Evaluation of dynamic tumour tracking radiotherapy with real-time monitoring for lung tumours using a gimbal mounted linac. Radiother Oncol. 2014;112(3):360–4.

2. 学会発表

① Y. Iizuka, N. Ueki, Y. Ishihara, M. Akimoto, H. Tanabe, K. Takayama, N. Mukumoto, M. Nakamura, Y. Miyabe, S. Kaneko, Y. Matsuo, T. Mizowaki, H. Monzen, A Sawada, M. Kokubo, M. Hiraoka. Evaluation of dose distribution and tracking accuracy in dynamic tumor-tracking irradiation for liver tumors using a gimbaled linac. ASTRO 56th annual meeting. Sep. 14-17, 2014. San Francisco, the US.

② 飯塚裕介、松尾幸憲、石原佳知、

秋元麻未、田邊裕朗、高山賢二、植木奈美、横田憲治、溝脇尚志、小久保雅樹、平岡眞寛. Vero4DRT を用いた肝腫瘍に対する動体追尾定位放射線治療（ポスター）日本放射線腫瘍学会 第 27 回学術大会平成 26 年 12 月 13 日. 横浜

③ 待鳥裕美子、木藤哲史、柴田友紀子、影山俊一郎、村田裕人、清水口卓也、田中寛、藤井元彰、二瓶圭二、唐澤克之. Vero4DRT による動体追尾照射を用いた肺定位放射線治療の初期経験（ポスター）日本放射線腫瘍学会 第 27 回学術大会平成 26 年 12 月 13 日. 横浜

G. 知的財産権の出願・登録状況(予定を含む)

1. 特許取得

なし

2. 実用新案登録

なし

3. その他

特になし

厚生労働科学研究委託費（革新的がん医療実用化研究事業）
委託業務成果報告

難治がんに対する動体追尾放射線治療の臨床評価に関する研究
業務項目：医学物理プロジェクト

担当責任者：中村　光宏　　京都大学医学部　講師

研究要旨
多施設共同試験では，臨床成績への影響が大きい放射線出力のばらつきおよび施設間における治療手順の違いを抑えることが重要である。本研究では、「第三者機関による治療装置の出力線量測定」および「施設間での治療手順の標準化」を実施した。
「第三者機関による治療装置の出力線量測定」では、全施設で合格通知を受け取った。
「施設間での治療手順の標準化および動体追尾精度の検証」では、施設間で治療手順に違いがあることが判明したため、治療手順の標準化を図り、プロトコールに反映した。

A. 研究目的

多施設共同試験では,臨床成績への影響が大きい放射線出力のばらつきおよび施設間における治療手順の違いを抑えることが重要である。本研究では、「第三者機関による治療装置の出力線量測定」および「施設間での治療手順の標準化」を実施する。

B. 研究方法

「第三者機関による治療装置の出力線量測定」と「施設間での治療手順の標準化および動体追尾精度の検証」を実施した。

前者では、米国放射線治療支援センター(http://rpc.mdanderson.org/RPC/home.htm)より人型不均質ファントムを借り入れ、共同試験に参加を表明している施設(京都大学医学部附属病院、先端医療センター、がん・感染症センター都立駒込病院、京都桂病院)に対して線量精度を検証した。後者では、プロトコール作成のための事前アンケートを実施した。

C. 研究結果

「第三者機関による治療装置の出力線量測定」では、全施設で合格通知を受け取った。

「施設間での治療手順の標準化および動体追尾精度の検証」では、施設間で治療手順に違いがあることが判明したため、治療手順の標準化を図り、プロトコールに反映した。

なお、症例登録が始まっていないため、動体追尾精度の検証は実施できていない。

D. 考察

出力線量測定結果より、共同試験に参加を表明している施設の線量計算精度は同等であることがわかった。また、治療手順を標準化したことで、動体追尾精度に施設間バイアスが除去されることが想定される。

E. 結論

多施設臨床試験を開始するために必要

な「第三者機関による治療装置の出力線量測定」および「施設間での治療手順の標準化」を実施した。

F. 研究発表

1. 論文発表

① Nakamura M, Akimoto M, Ono T, Nakamura A, Kishi T, Yano S, Nakata M, Itasaka S, Mizowaki T, Shibuya K, Hiraoka M. Interfraction Positional Variation in Pancreatic Tumors using Daily Breath-hold Cone-beam Computed Tomography with Visual Feedback. J Appl Clin Med Phys. (in press).

② Akimoto M, Nakamura M, Mukumoto N, Yamada M, Tanabe H, Ueki N, Kaneko S, Matsuo Y, Mizowaki T, Kokubo M, Hiraoka M. Baseline correction of a correlation model for improving the prediction accuracy of infrared marker-based dynamic tumor tracking. J Appl Clin Med Phys. (in press).

③ Nakamura M, Akimoto M, Mukumoto N, Yamada M,Tanabe H, Ueki N, Matsuo Y, Mizowaki T, Kokubo M,Hiraoka M. Influence of the correlation modeling period on the prediction accuracy of infrared marker-based dynamic tumor tracking using a gimbaled X-ray head. Physica Medica, 2015 (in press).

④ Ishihara Y, Sawada A, Nakamura M, Miyabe Y, Tanabe H, Kaneko S, Takayama K, Mizowaki T, Kokubo M, Hiraoka M. Development of a dose verification system for Vero4DRT using Monte Carlo method. J Appl Clin Med Phys. 2014;15:160-172

⑤ Shiinoki T, Sawada A, Ishihara Y, Miyabe Y, Matsuo Y, Mizowaki T, Kokubo M, Hiraoka M. Dosimetric impact of gold markers implanted closely to lung tumors: a Monte Carlo simulation. J Appl Clin Med Phys. 2014;15:71-79.

2. 学会発表

① 木藤哲史、岡野智行、橋本俊信、米川五朗、古谷智久、橋本慎平、二瓶圭二、唐澤克之. 4 次元放射線治療における基準マーカ位置の評価方法(口頭) 日本放射線腫瘍学会 第 27 回学術大会平成 26 年 12 月 13 日. 横浜

G. 知的財産権の出願・登録状況(予定を含む)

1. 特許取得

なし

2. 実用新案登録

なし

3. その他

なし

様式第１９

学　会　等　発　表　実　績

委託業務題目「難治がんに対する動体追尾放射線治療の臨床評価に関する研究」
機関名　国立大学法人京都大学

１．学会等における口頭・ポスター発表

発表した成果（発表題目、口頭・ポスター発表の別）	発表者氏名	発表した場所（学会等名）	発表した時期	国内・外の別
Evaluation of dose distribution and tracking accuracy in dynamic tumor-tracking irradiation for liver tumors using a gimbaled linac.（ポスター）	Y. Iizuka, N. Ueki, Y. Ishihara, M. Akimoto, H. Tanabe, K. Takayama, N. Mukumoto, M. Nakamura, Y. Miyabe, S. Kaneko, Y. Matsuo, T. Mizowaki, H. Monzen, A Sawada, M. Kokubo, M. Hiraoka.	ASTRO 56th annual meeting.	平成26年9月14～17日	国外
Vero4DRTを用いた肝腫瘍に対する動体追尾定位放射線治療（ポスター）	飯塚裕介、松尾幸憲、石原佳知、秋元麻未、田邊裕朗、高山賢二、植木奈美、横田憲治、溝脇尚志、小久保雅樹、平岡眞寛.	日本放射線腫瘍学会第27回学術大会	平成26年12月13日	国内
Vero4DRTによる動体追尾照射を用いた肺定位放射線治療の初期経験（ポスター）	待鳥裕美子、木藤哲史、柴田友紀子、影山俊一郎、村田裕人、清水口卓也、田中寛、藤井元彰、二瓶圭二、唐澤克之.	日本放射線腫瘍学会第27回学術大会	平成26年12月13日	国内
4次元放射線治療における基準マーカ位置の評価方法（口頭）	木藤哲史、岡野智行、橋本俊信、米川五朗、古谷智久、橋本慎平、二瓶圭二、唐澤克之.	日本放射線腫瘍学会第27回学術大会	平成26年12月13日	国内

２．学会誌・雑誌等における論文掲載

掲載した論文（発表題目）	発表者氏名	発表した場所 （学会誌・雑誌等名）	発表した時期	国内・外の別
Interfraction Positional Variation in Pancreatic Tumors using Daily Breath-hold Cone-beam Computed Tomography with Visual Feedback.	Nakamura M, Akimoto M, Ono T, Nakamura A, Kishi T, Yano S, Nakata M, Itasaka S, Mizowaki T, Shibuya K, Hiraoka M.	J Appl Clin Med Phys.	(in press).	国外
Baseline correction of a correlation model for improving the prediction accuracy of infrared marker-based dynamic tumor tracking.	Akimoto M, Nakamura M, Mukumoto N, Yamada M, Tanabe H, Ueki N, Kaneko S, Matsuo Y, Mizowaki T, Kokubo M, Hiraoka M.	J Appl Clin Med Phys.	(in press).	国外
Influence of the correlation modeling period on the prediction accuracy of infrared marker-based dynamic tumor tracking using a gimbaled X-ray head.	Nakamura M, Akimoto M, Mukumoto N, Yamada M, Tanabe H, Ueki N, Matsuo Y, Mizowaki T, Kokubo M, Hiraoka M.	Physica Medica	(in press).	国外
Stereotactic body radiotherapy for synchronous primary lung cancer: clinical outcome of 18 cases.	Shintani T, Masago K, Takayama K, Ueki K, Kimino G, Kosaka Y, Imagumbai T, Katakami N, Kokubo M.	Clinical Lung Cancer	(in press).	国外

Comparison of long-term survival outcomes between stereotactic body radiotherapy and sublobar resection for stage I non-small-cell lung cancer in patients at high risk for lobectomy: A propensity score matching analysis.	Matsuo Y, Chen F, Hamaji M, Kawaguchi A, Ueki N, Nagata Y, Sonobe M, Morita S, Date H, Hiraoka M.	Eur J Cancer.	2014	国外
Evaluation of dynamic tumour tracking radiotherapy with real-time monitoring for lung tumours using a gimbal mounted linac.	Matsuo Y, Ueki N, Takayama K, Nakamura M, Miyabe Y, Ishihara Y, Mukumoto N, Yano S, Tanabe H, Kaneko S, Mizowaki T, Monzen H, Sawada A, Kokubo M, Hiraoka M.	Radiother Oncol.	2014	国外
Development of a dose verification system for Vero4DRT using Monte Carlo method.	Ishihara Y, Sawada A, Nakamura M, Miyabe Y, Tanabe H, Kaneko S, Takayama K, Mizowaki T, Kokubo M, Hiraoka M.	J Appl Clin Med Phys.	2014	国外
Dosimetric impact of gold markers implanted closely to lung tumors: a Monte Carlo simulation.	Shiinoki T, Sawada A, Ishihara Y, Miyabe Y, Matsuo Y, Mizowaki T, Kokubo M, Hiraoka M.	J Appl Clin Med Phys.	2014	国外

研究成果の刊行物・別刷

Physica Medica xxx (2015) 1–6

Contents lists available at ScienceDirect

Physica Medica

journal homepage: http://www.physicamedica.com

Original paper

Influence of the correlation modeling period on the prediction accuracy of infrared marker-based dynamic tumor tracking using a gimbaled X-ray head

Mitsuhiro Nakamura [a,*], Mami Akimoto [a], Nobutaka Mukumoto [a], Masahiro Yamada [a], Hiroaki Tanabe [b], Nami Ueki [a], Yukinori Matsuo [a], Takashi Mizowaki [a], Masaki Kokubo [c], Masahiro Hiraoka [a]

[a] Department of Radiation Oncology and Image-Applied Therapy, Graduate School of Medicine, Kyoto University, Japan
[b] Division of Radiation Oncology, Institute of Biomedical Research and Innovation, Japan
[c] Department of Radiation Oncology, Kobe City Medical Center General Hospital, Japan

ARTICLE INFO

Article history:
Received 7 November 2014
Received in revised form
10 January 2015
Accepted 12 January 2015
Available online xxx

Keywords:
Vero4DRT
IR tracking
Modeling period
Prediction accuracy

ABSTRACT

Purpose: To assess the utility of 10 s and 20 s modeling periods, rather than the 40 s currently used, in the clinical construction of practical correlation models (CMs) in dynamic tumor tracking irradiation using the Vero4DRT.

Methods: The CMs with five independent parameters (CM parameters) were analyzed retrospectively for 10 consecutive lung cancer patients. CM remodeling was performed two or three times per treatment session. Three different CMs trained over modeling periods of 10, 20, and 40 s were built from a single, original CM log file. The predicted target positions were calculated from the CM parameters and the vertical displacement of infrared markers on the abdomen (P_{IR}) during the modeling. We assessed how the CM parameters obtained over modeling periods of T s (T = 10, 20, and 40 s) were robust to changes in respiratory patterns after several minutes. The mimic-predicted target positions after several minutes were computed based on the previous CM parameters and P_{IR} during the next modeling. The 95th percentiles of the differences between mimic-predicted and detected target positions over 40 s ($E95_{robust,T}$: T = 10, 20, and 40 s) were then calculated.

Results: Strong correlations greater than 0.92 were observed between the $E95_{robust,20}$ and $E95_{robust,40}$ values. Meanwhile, irregular respiratory patterns with inconsistent amplitudes of motion created differences between the $E95_{robust,10}$ and $E95_{robust,40}$ values of ≥10 mm.

Conclusions: The accuracies of CMs derived using 20 s were almost identical to those obtained over 40 s, and superior to those obtained over 10 s.

Introduction

Respiratory motion creates uncertainty during beam delivery. If such motion is not managed, large margins should be added to clinical target volumes [1]. Several investigators have reported that use of large target volumes increased complications in normal tissues in lung and pancreatic cancer patients [2,3]. Management of respiratory motion is effective in reducing beam delivery to normal tissue, in turn, making it possible to escalate the dose to the tumor.

Respiration-synchronized beam delivery techniques that are used clinically to reduce the impact of respiratory motion can be separated broadly into three categories: breath-holding, respiratory gating, and dynamic tumor tracking (DTT) [4,5]. Of these, recent interest has focused on the DTT technique, which can be used to reposition the radiation beam dynamically with reference to the target position. Compared with breath-holding and respiratory gating, DTT can minimize the internal margins while maintaining a 100% duty cycle. This delivers the beam efficiently without the need for patients to hold their breath.

We have applied infrared (IR) marker-based DTT irradiation (IR Tracking) clinically using the Vero4DRT (Mitsubishi Heavy Industries [MHI], Ltd., Tokyo, Japan, and Brainlab AG, Feldkirchen, Germany) in treating lung cancer patients since September 2011

* Corresponding author. Kyoto University, Graduate School of Medicine, 54 Kawahara-cho, Shogoin, Sakyo-ku, Kyoto 606-8507, Japan.
E-mail address: m_nkmr@kuhp.kyoto-u.ac.jp (M. Nakamura).

http://dx.doi.org/10.1016/j.ejmp.2015.01.004
1120-1797/

[6–10]. IR Tracking is categorized as a hybrid DTT method that combines direct localization methods with an indirect DTT method [11]. IR Tracking observes external surrogate features and determines localization of the internal target using a correlation model (CM) derived from both one-dimensional (1D) surrogate data and 3D internal target data. A key issue in IR Tracking is the accuracy of the CM used [4,11]. A CM affected by poor precision will increase localization error. Before starting IR Tracking at each fraction, the vertical displacement of IR markers on the abdomen and the 3D position of a tumor, as indicated by implanted fiducial markers (detected target positions), are monitored for 20, 30, or 40 s to build a CM (Fig. 1). Vero4DRT users can select the training periods. We have used a modeling period of 40 s to acquire as much information as possible on the respiratory pattern. The 3D-predicted target position is then calculated during treatment, based on 1D surrogate data and the CM.

There are several reports on the tracking accuracy of IR Tracking. Mukumoto et al. [9] found that the 95th percentiles of overall targeting errors were up to 4.1 mm when a modeling period of 40 s was used. Depuydt et al. [12] typically used a modeling period of 20 s in a patient simulation study. However, these studies did not address the influence of different modeling periods on tracking accuracy. Also, our group has previously concluded that changes in breathing patterns, including baseline drift, reduced the correlation between internal target and external IR marker positions [8]. As a next step, based on those previous results, we believed that the modeling period could greatly influence the tracking accuracy.

The purpose of the present study was to compare the prediction accuracy using modeling periods of 10 and 20 s, rather than the 40 s currently used in the clinical construction of practical CMs in IR Tracking.

Materials and methods

Patients

We analyzed CMs retrospectively over a modeling period of 40 s for 10 consecutive lung cancer patients who underwent IR Tracking. Five patients were treated at Kyoto University Hospital and five at the Institute of Biomedical Research and Innovation. There were eight male patients and two females, with a median age of 85 (range, 60–87) years. Lung tumors were located in the right middle lobe (one patient), in the right lower lobe (six), and in the left lower lobe (three). Four or five fiducial markers, 1.5 mm in diameter, were implanted transbronchially around the lung tumor. An individualized vacuum pillow (Kyoto University Hospital: Bodyfix; Medical Intelligence, Schwabmünchen, Germany; Institute of Biomedical Research and Innovation: ESFORM Engineering System, Matsumoto, Japan) was made for each patient with both arms raised. Five IR markers were attached to the abdominal wall to allow monitoring of external respiratory signals. A CM remodeling was performed two or three times per treatment session to improve the prediction accuracy, and the median elapsed time prior to remodeling was 12 (range, 2–33) min.

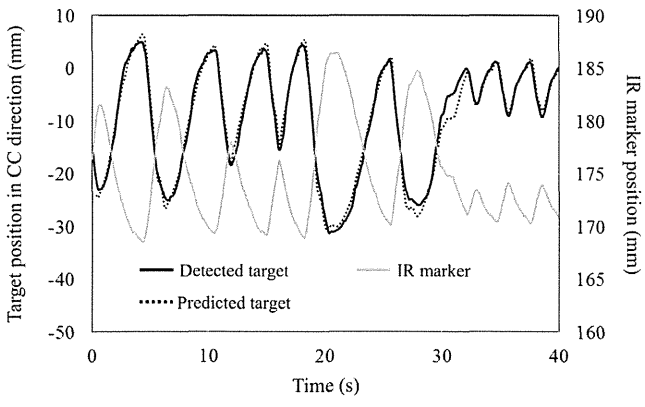

Figure 1. An example of a representative CM. The detected and predicted target positions in the CC direction and IR marker positions are shown.

In clinical practice, we monitored the implanted fiducial markers at a minimum monitoring interval of 1 s during beam delivery via orthogonal kV X-ray imaging. Circles with user-defined radii (3 mm at our hospital), placed around the predicted positions of the fiducial markers (tolerance circles), were displayed on monitor images to serve as benchmarks for CM remodeling. Vero4DRT does not support an auto CM updating function; thus, additional correlation modeling was needed to improve prediction accuracy during each treatment session if any systematic deviation between the positions of the fiducial markers and the tolerance circles was observed [8,9].

Calculating the predicted target position

Immediately after correction of any initial setup error caused by bony anatomy, an ExacTrac subsystem integrated into the Vero4DRT platform constructed a CM over a modeling period of 40 s. During the modeling period, the vertical displacement of IR markers on the abdomen (P_{IR}) values and the implanted fiducial markers were monitored simultaneously with an IR camera at 60 Hz and with an orthogonal kV X-ray imaging subsystem at 6.25 or 12.5 Hz. The sampling frequency changed automatically from 12.5 to 6.25 Hz when the velocity of IR marker motion (v_{IR}) decreased. The monitoring interval of 1 s remains the same, independent of the sampling frequency. The gantry and ring angle used for monitoring of implanted fiducial markers were determined with reference to the findings of our previous study [6]. In total, ~500-kV X-ray fluoroscopic image sets were acquired during a single correlation modeling session over 40 s. The imaging parameters were 110 kV, 100 mA, and 5 or 10 ms. These settings are the minima required to detect implanted fiducials in lung cancer cases. The CM was expressed using a quadratic function in terms of P_{IR} and v_{IR}, as follows:

$$F(P_{IR}, v_{IR}) = aP_{IR}^2 + bP_{IR} + c + dv_{IR}^2 + ev_{IR} \quad (1)$$

Three different CMs with modeling periods of 10, 20, and 40 s were constructed retrospectively from original CM log files using software developed in-house. The 10- and 20-s modeling periods were extracted from the beginning of the 40-s modeling period.

Based on available information from the vendor, the CM was built as following 1–4:

1. The predicted P_{IR} after 25 ms $[P'_{IR,k}(t+25)]$ was calculated from the previous multiple consecutive positions of the kth IR marker ($P_{IR,k}$; $1 \le k \le 5$) before time t, using an approximate linear equation derived using the weighted least-squares method. A time of 25 ms was required to compensate for the sub-system latency of IR marker position acquisition. Depuydt et al. [13] mentioned sub-system latencies in terms of the IR marker position acquisition of 25 ms. We were also informed of the latency of IR marker position acquisition by MHI and Brainlab AG. Details of the construction and the stability of the weighted least-squares model cannot be disclosed because of a provision in our contract with MHI and Brainlab AG.

Please cite this article in press as: Nakamura M, et al., Influence of the correlation modeling period on the prediction accuracy of infrared marker-based dynamic tumor tracking using a gimbaled X-ray head, Physica Medica (2015), http://dx.doi.org/10.1016/j.ejmp.2015.01.004

2. The velocity at time $t + 25$ ms $[v'_{IR,k}(t + 25)]$ was calculated from $P_{IR,k}$ and $P'_{IR,k}$, assuming that the velocity was constant between t and $t + 25$ ms.
3. Optimal CM parameters (a_k, b_k, c_k, d_k, and e_k) were determined, via multiple regression analysis that derives an optimal solution, by minimizing the residual errors between detected target positions on the kV X-ray fluoroscopic images (P_D) and tentative target positions predicted from the displacement of the kth IR marker.
4. The CM was built after the above processes were repeated for each IR marker.

During the beam delivery, each target position predicted from displacement of the kth IR marker was calculated using the parameters of the corresponding CM, and the mean value of the predicted target position, calculated from the displacement of the kth IR marker, served as the predicted target position (P_P).

Comparison of detected target positions with predicted target positions

First, we assessed whether use of a shorter modeling period allowed creation of a CM of a high degree of goodness-of-fit during modeling periods of T s (T = 10, 20 and 40 s). The differences between P_P and P_D at each sampling point during modeling periods of T s ($E_{fit,T}$: T = 10, 20 and 40 s) were calculated during modeling periods of T s (T = 10, 20 and 40 s). In total, 255 CMs (85 log files × three different modeling periods) were analyzed.

Next, CM parameters obtained over modeling periods of 10, 20, and 40 s were input with P_{IR} values collected for 40 s during the next modeling, and mimic P_P (P'_P) was then computed using Eq. (1). Subsequently, the differences between P'_P and P_D observed during the next modeling over 40 s ($E_{robust,T}$: T = 10, 20 and 40 s) at each sampling point were calculated. The zero value of $E_{robust,T}$ (T = 10 and 20 s) − $E_{robust,40}$ indicated that the robustness of CM parameters obtained over modeling periods of T s (T = 10 and 20 s) was identical to those over 40 s. In total, 42 paired CM log files were analyzed. Fig. 2 shows a schematic workflow of $E_{fit,T}$ and $E_{robust,T}$ (T = 10, 20 and 40 s) calculations. Analysis of variance (ANOVA) was used to assess the hypotheses that there was no difference in $E_{fit,T}$ and $E_{robust,T}$ (T = 10, 20 and 40 s) between the three different modeling periods.

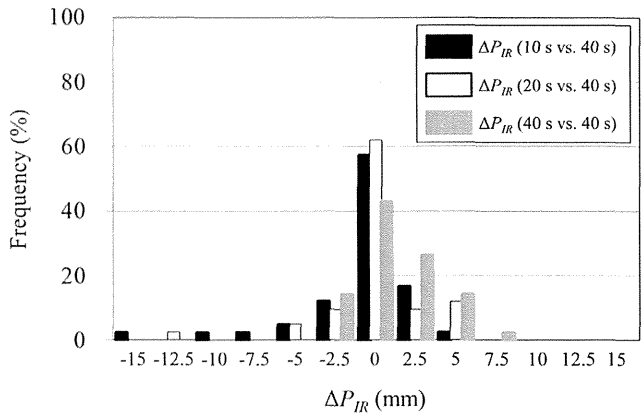

Figure 3. Distributions of differences between the maximum amplitudes of P_{IR} (the ΔP_{IR} values) for a modeling period of 10, 20 or 40 s in the previous modeling, and those for 40 s in the next modeling. Positive values indicate that the maximum amplitudes of P_{IR} in the previous modeling were larger than those in the next modeling.

Results

Characteristics of respiratory patterns

The median peak-to-peak amplitude of P_D were in the ranges 0.2–5.6 mm, 1.4–23.5 mm, and 0.9–6.6 mm in the left-right (LR), cranio-caudal (CC), and anterior-posterior (AP) directions, respectively. A modeling period of 10 s included at least one breathing cycle. The median breathing cycle numbers within modeling periods of 10, 20, and 40 s were 3 (range, 1–4), 6 (range, 2–8), and 11 (range, 4–16), respectively. Fig. 3 shows how the maximum amplitudes of P_{IR} (the ΔP_{IR} values) changed between the previous and next modeling period. Positive values indicate that the maximum amplitudes of P_{IR} in the previous modeling were larger than those in the next modeling. The ΔP_{IR} values of over −5 mm were not observed for a modeling period of 40 s in the previous modeling.

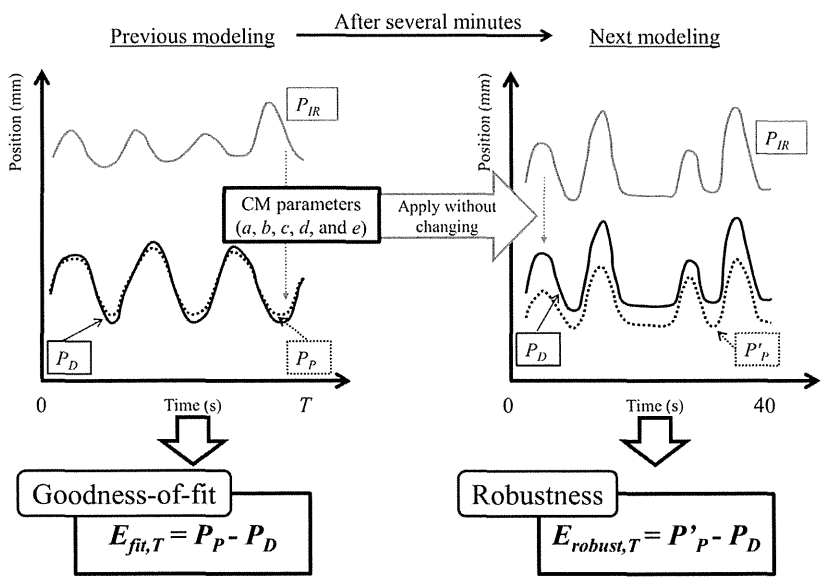

Figure 2. Schematic diagram showing how $E_{fit,T}$ and $E_{robust,T}$ (T = 10, 20 and 40 s) were calculated.

Please cite this article in press as: Nakamura M, et al., Influence of the correlation modeling period on the prediction accuracy of infrared marker-based dynamic tumor tracking using a gimbaled X-ray head, Physica Medica (2015), http://dx.doi.org/10.1016/j.ejmp.2015.01.004

Table 1
Means ± standard deviations of $E_{fit,T}$ values and the proportions of absolute $E_{fit,T}$ values <1 mm. The latter figures are shown in parentheses.

	LR	CC	AP
$E_{fit,10}$	0.0 ± 0.3 mm (98.3%)	0.0 ± 0.6 mm (89.6%)	0.0 ± 0.5 mm (94.5%)
$E_{fit,20}$	0.0 ± 0.3 mm (98.9%)	0.0 ± 0.7 mm (93.7%)	0.0 ± 0.6 mm (96.5%)
$E_{fit,40}$	0.0 ± 0.4 mm (96.7%)	0.0 ± 0.7 mm (83.7%)	0.0 ± 0.6 mm (90.7%)

Abbreviations: LR, left–right; CC, cranial–caudal; AP, anterior–posterior.

Accuracy of predicted target positions by modeling period

In this subsection, the results of $E_{fit,T}$, defined as the differences between P_P and P_D at each sampling point during modeling periods of T s (T = 10, 20 and 40 s), were summarized. Means ± standard deviations (SDs) of the $E_{fit,T}$ values, and the proportions of absolute $E_{fit,T}$ values <1 mm are shown in Table 1. The means ± SDs of $E_{fit,T}$ values and the proportions of absolute $E_{fit,T}$ values <1 mm over modeling periods of 10 and 20 s were comparable to those obtained over 40 s. The 3D SD was 0.6 mm for $E_{fit,10}$, $E_{fit,20}$, and $E_{fit,40}$. ANOVA revealed no significant difference between $E_{fit,10}$, $E_{fit,20}$, and $E_{fit,40}$.

Robustness of prediction accuracies using the correlation modeling parameters obtained in the previous modeling

In this subsection, the results of $E_{robust,T}$ (T = 10, 20 and 40 s), defined as the differences between P'_P and P_D during the next modeling over 40 s, are summarized. Table 2 shows the maximum values of 95th percentiles of $E_{robust,10}$ ($E95_{robust,10}$), $E_{robust,20}$ ($E95_{robust,20}$), and $E_{robust,40}$ ($E95_{robust,40}$) in each patient. Fig. 4 shows distributions of difference between $E95_{robust,10}$ or $E95_{robust,20}$ and $E95_{robust,40}$ for every fraction. No absolute difference between $E95_{robust,20}$ and $E95_{robust,40}$ of over 3 mm was observed, and high correlation coefficients were observed between the $E95_{robust,20}$ and $E95_{robust,40}$ values in all three directions (LR: R = 0.92; CC: R = 0.92; and AP: R = 0.94). Meanwhile, the absolute difference between $E95_{robust,10}$ and $E95_{robust,40}$ of over 3 mm was observed in two fractions (4.8%), which provided the low correlation coefficients between the $E95_{robust,10}$ and $E95_{robust,40}$ values (LR: R = 0.55; CC: R = 0.64; and AP: R = 0.62); however, the correlation coefficients became strong (LR: R = 0.97; CC: R = 0.89; and AP: R = 0.93), excluding these two fractions. The combination of Tables 1 and 2 also shows that the breathing patterns in the previous modeling differed from those in the next modeling, particularly for patient #8 with the largest difference. Fig. 5 shows the P_{IR} pattern in the next modeling and the $E_{robust,10}$, $E_{robust,20}$, and $E_{robust,40}$ values for patient #8 in the AP direction. As shown in Fig. 5, the maximum P_{IR} measured over 10 and 20 s in the previous modeling was considerably smaller than that over 40 s in the next modeling, whereas the maximum P_{IR} derived over 40 s in the previous modeling exceeded the upper limit of P_{IR} obtained in the next modeling. The $E_{robust,10}$ and $E_{robust,20}$ values were more pronounced at the peak positions where the maximum amplitudes of P_{IR} for 10 and 20 s in the previous modeling did not exceed those in the next modeling over 40 s. High negative correlations were observed between $E_{robust,10}$ and P_{IR} collected in the next modeling (R = −0.89), and between $E_{robust,20}$ and P_{IR} collected in the next modeling (R = −0.89).

Fig. 6 shows the relationship between ΔP_{IR} and $E_{robust,T}$−$E_{robust,40}$ (T = 10 and 20 s). The negative value of ΔP_{IR} indicated that the maximum amplitudes of P_{IR} for a modeling period of 10 s or 20 s in the previous modeling were smaller than those for 40 s in the next modeling. The difference between $E95_{robust,T}$ and $E95_{robust,40}$ values became more pronounced when the ΔP_{IR} was large. In the group with the modeling period over 20 s in the previous modeling, the SDs of differences between the $E95_{robust,10}$ and $E95_{robust,40}$ values were 0.3, 0.4, and 0.5 mm in the LR, CC, and AP directions, respectively Fig. 6(a). In the group with the modeling period over 10 s in the previous modeling, the SDs were 1.3, 1.0, and 2.0 mm in the LR, CC, and AP directions, respectively Fig. 6(b).

Discussion

Exact 3D prediction of the target position is important in DTT irradiation, and many reports regarding prediction accuracy for several modalities have been published [7–16]. According to the available information from the vendor, we compensated for the latency of the IR marker position acquisition of 25 ms to construct the CM; however, sub-systems other than the IR system, including motion of the gimbals head, also have latency. We have previously shown that the Vero4DRT system can construct highly accurate CMs in both phantom and clinical studies [7–9]. Another group showed that the Vero4DRT performed excellently when used in the DTT mode [13], and the Vero4DRT DTT function was equivalent to that of other clinical DTT systems in a patient simulation study [12]. From these results, the latency for other sub-systems could be negligible.

The Synchrony system, a component of the CyberKnife Robotic Radiosurgery platform (Accuracy Inc., Sunnyvale, CA), requires a CM composed of various breathing cycles, prior to beam delivery [17,18]. Clinically selectable modeling periods for Vero4DRT also include several breathing cycles. In the current study, we focused on the availability of 10 s modeling periods, which included at least one breathing cycle.

For the CM goodness-of-fit during modeling periods of T s (T = 10, 20 and 40 s), we found that means ± SDs of the $E_{fit,10}$ and $E_{fit,20}$ were comparable to those of $E_{fit,40}$, indicating that a successful CM fit was obtained even when the respiratory pattern was monitored for 10 or 20 s. According to Hoogeman et al. [18], the

Table 2
Maximum value of $E95_{robust,10}$, $E95_{robust,20}$ and $E95_{robust,40}$ in each patient.

Patient	LR (mm)			CC (mm)			AP (mm)		
	$E95_{robust,10}$	$E95_{robust,20}$	$E95_{robust,40}$	$E95_{robust,10}$	$E95_{robust,20}$	$E95_{robust,40}$	$E95_{robust,10}$	$E95_{robust,20}$	$E95_{robust,40}$
1	0.5	0.5	0.5	2.5	2.5	2.3	2.3	2.4	2.4
2	1.9	2.0	1.8	4.6	4.6	4.7	2.0	2.0	1.9
3	1.1	1.0	1.0	4.7	4.5	4.2	2.5	2.1	2.1
4	0.5	0.5	0.5	2.8	2.5	2.7	1.2	1.1	1.2
5	1.3	1.3	1.3	3.6	3.4	3.4	6.2	6.2	5.9
6	2.2	2.1	2.1	1.9	1.8	1.6	3.0	2.8	2.8
7	1.2	1.2	1.2	3.1	3.3	3.7	1.4	1.4	1.5
8	9.9	3.2	2.6	8.3	4.8	5.3	14.3	4.6	4.0
9	0.6	0.6	0.5	3.2	3.3	2.9	0.8	0.7	0.7
10	1.5	1.5	1.4	4.7	4.7	4.6	2.1	2.0	2.1

Abbreviations: LR, left–right; CC, cranial–caudal; AP, anterior–posterior.

Please cite this article in press as: Nakamura M, et al., Influence of the correlation modeling period on the prediction accuracy of infrared marker-based dynamic tumor tracking using a gimbaled X-ray head, Physica Medica (2015), http://dx.doi.org/10.1016/j.ejmp.2015.01.004

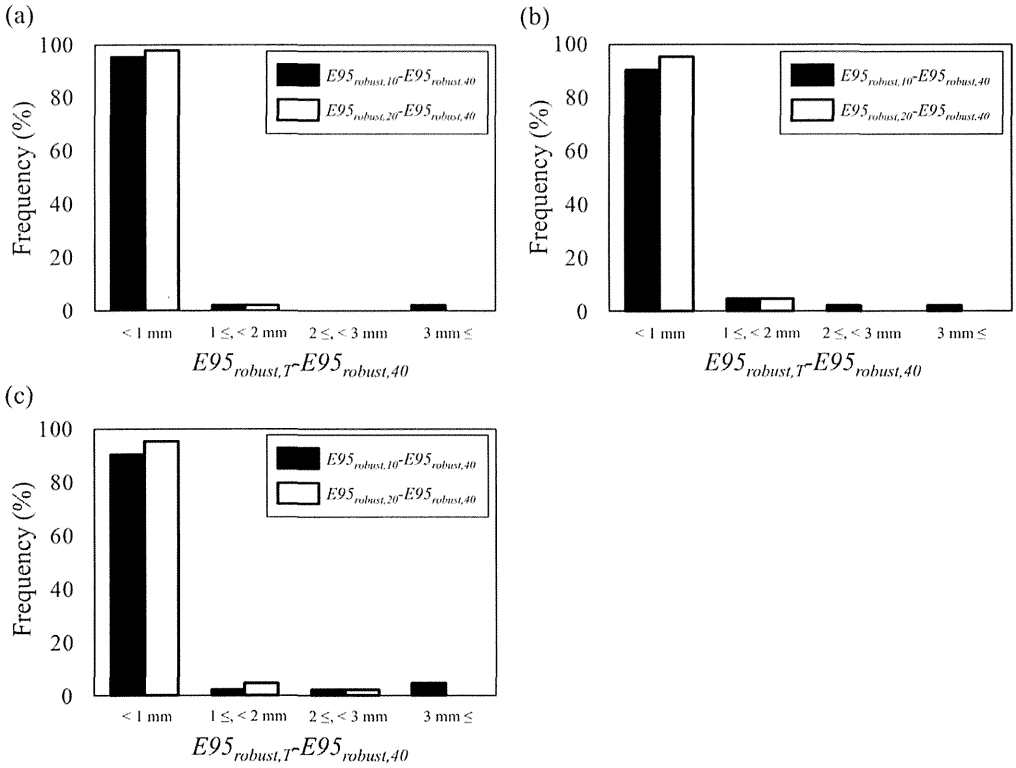

Figure 4. Distributions of $E95_{robust,10}$-$E95_{robust,40}$ (black bar) and $E95_{robust,20}$-$E95_{robust,40}$ (white bar) in the (a) LR, (b) CC, and (c) AP directions.

correlation model fit error had low mean values and an SD of 0.3 mm, which is comparable with our results.

The Synchrony system constantly updates its CM as each new X-ray image is acquired, periodically correcting for any change in a patient's breathing patterns. Hoogeman et al. also showed that the correlation model errors in the absence of Synchrony were up to 8.1 mm, suggesting the importance of the use of respiratory motion tracking [18]. The current software version of the Vero4DRT cannot automatically update the CM without stopping beam delivery, prolonging treatment time. However, CM re-modeling is required to ensure the prediction accuracy during treatment. Thus, the robustness of CM parameters is of clinical importance. We found that breathing patterns in the previous modeling differed from those in the next modeling. While the percentages of $E95_{robust,20}$-$E95_{robust,40}$ <1 mm were greater than 95% in each direction, $E95_{robust,10}$ values over 3 mm were occasionally observed for the modeling period of 10 s in the previous modeling (Fig. 4). Fig. 5 demonstrates that irregular respiratory patterns with inconsistent amplitudes of motion created differences between the $E_{robust,10}$ and $E_{robust,40}$ values of ≥10 mm. A possible reason for this was that the CM might not correctly extrapolate beyond the observed input range or if the trajectory of the tumor changed dramatically for large amplitudes. Fig. 6 shows that a greater ΔP_{IR} is potentially associated with large prediction errors. In the current study, the 10- and 20-s modeling periods were taken in the beginning of the 40-s modeling period. Because there are many ways to extract 10 and 20 s from 40 s, taking the 10- and 20-s modeling periods later in the 40-s modeling period would change the results. Therefore, regardless of the modeling period, it is important for the patient to breathe regularly to ensure high accuracy during IR Tracking. Based on the findings of the current study, a minimum modeling period of 20 s should be used for following DTT patients.

Our results are useful in terms of reducing the imaging dose. Our group experimentally measured the dose as ~0.1 mGy per image [19], essentially the same as that of the Synchrony system [20]. However, hot spots with maximum imaging doses of 37.12 mGy were estimated during construction of a single CM over a modeling period of 40 s. When such a model is acquired three times, at the same monitoring angle, to ensure tracking accuracy during delivery of a single fraction, a maximum imaging dose of >0.4 Gy is at least theoretically attained over a four-fraction course of treatment, creating potential health hazards, including skin injuries and

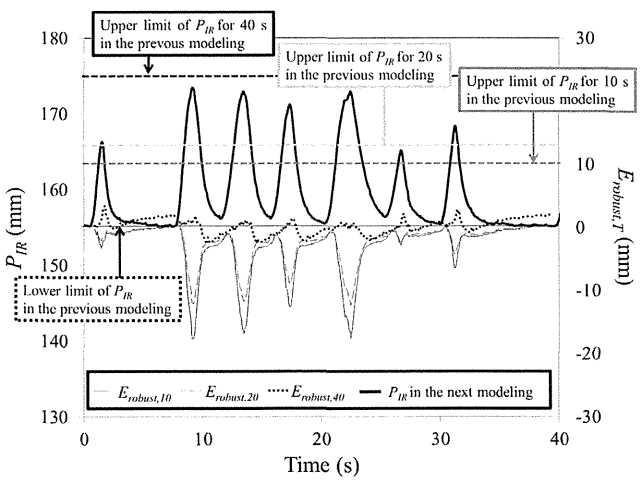

Figure 5. The P_{IR} pattern in the next modeling and the $E_{robust,10}$ (solid gray), $E_{robust,20}$ (broken gray), and $E_{robust,40}$ (broken black) data for patient #8, who had the largest difference between the $E95_{robust,10}$ and $E95_{robust,40}$ values in the AP direction.

Please cite this article in press as: Nakamura M, et al., Influence of the correlation modeling period on the prediction accuracy of infrared marker-based dynamic tumor tracking using a gimbaled X-ray head, Physica Medica (2015), http://dx.doi.org/10.1016/j.ejmp.2015.01.004